



## Original articles

Research article

<https://doi.org/10.17308/kcmf.2024.26/11938>

## Coupling of anode reactions in the process of electrooxidation of glycine anion on gold

I. D. Zartsyn, A. V. Vvedensky, E. V. Bobrinskaya✉, O. A. Kozaderov

Voronezh State University,  
1 Universitetskaya pl., Voronezh 394018, Russian Federation

## Abstract

Electrochemical processes involving organic substances are complex multi-stage reactions. In our opinion, it is incorrect to describe their kinetics using the principle of independent partial processes (or their individual stages) since electrode reactions can be coupled due to competition for active surface sites, due to common intermediate stages, or through an electron. In this case, the theory of coupled reactions or the graph-kinetic method should be used to provide the kinetic description of the process. In general, graph theory makes it possible to identify the relationship between the “structure” and the kinetic behavior of complex systems by means of graphical analysis. In the case of electrochemical reactions, structural elements are substances adsorbed on the metal surface and (or) a set of substances interacting in the reactions. The relationship between their concentrations can be characterized quantitatively by a transformation law, for example, the law of effective masses. Thus, a graph is a set of reacting substances and a sequence of reactions represented graphically. Graphs allow setting a system of kinetic equations and analyzing them by associating a certain behavior of the system with the structure of the corresponding graph. Under the assumption that one intermediate particle is involved in each elementary stage, the kinetic expressions will be linear, which corresponds to the first-order reaction model.

Graph-kinetic analysis of the processes within the  $\text{Au|Gly}^-, \text{OH}^-, \text{H}_2\text{O}$  system confirmed that the partial multi-stage reactions of anode oxidation of glycine and hydroxyl anions are kinetically coupled. We obtained expressions for partial currents of electrooxidation of hydroxide ions and glycine anions during the anodic process occurring on gold in an alkaline glycine-containing solution. It was shown that with an increase in the anode potential, the nature of the limiting stage of the anodic process changes.

Formal constants of rates and equilibria of electrochemical reactions involving particles of background electrolyte and glycinate ion were calculated. It was found that the rates of partial oxidation reactions of adsorbed  $\text{OH}$  particles and  $\text{OH}^-$  are significantly higher than those of organic anions ( $\text{Gly}^-$  and  $\text{HCOO}^-$ ). This indicates that the kinetics of the electrooxidation processes of  $\text{Gly}^-$  in the  $\text{Au|Gly}^-, \text{OH}^-, \text{H}_2\text{O}$  system are determined by the kinetic features of the electrooxidation reactions of hydroxide ions.

**Keywords:** Graph-kinetic analysis, Coupled processes, Electrooxidation, Glycine, Voltammetry

**Funding:** The study was supported by the Ministry of Science and Higher Education of the Russian Federation within the framework of state order to higher education institutions in the sphere of scientific research for 2022-2024, project № FZGU-2022-0003.

**For citation:** Zartsyn I. D., Vvedenskii A. V., Bobrinskaya E. V., Kozaderov O. A. Coupling of anode reactions in the process of electrooxidation of glycine anion on gold. *Condensed Matter and Interphases*. 2024;26(2): 253–264. <https://doi.org/10.17308/kcmf.2024.26/11938>

**Для цитирования:** Зарцын И. Д., Введенский А. В., Бобринская Е. В., Козадегов О. А. Сопряжение анодных реакций в процессе электроокисления аниона глицина на золоте. *Конденсированные среды и межфазные границы*. 2024;26(2): 253–264. <https://doi.org/10.17308/kcmf.2024.26/11938>

✉ Bobrinskaya Elena Valerievna, e-mail: [elena173.68@mail.ru](mailto:elena173.68@mail.ru)

© Zartsyn I. D., Vvedenskii A. V., Bobrinskaya E. V., Kozaderov O. A., 2024



The content is available under Creative Commons Attribution 4.0 License.

## 1. Introduction

When several multi-stage processes occur on the surface of the electrode, they can be interconnected through intermediate particles (intermediates) and thus influence each other. In this case, the kinetics of the electrode reaction should be described using the graph method, which is often used to analyze enzymatic reactions in biochemistry [1–4]. In general, graph theory makes it possible to identify the relationship between the “structure” and the kinetic behavior of complex systems by means of graphical analysis. In this case, the “structure” is understood as the interaction and relationship between the elements of a given system, and its behavior is described by analyzing its response to an external disturbance. The partial and total  $i,E$ -dependencies are calculated by sequentially considering various kinetic situations that differ in the assumption about the nature of the limiting stage or take into account the presence of several slow stages with comparable rates. Comparing the total  $i,E$ -dependency with the experimental polarization  $i,E$ -curve allows drawing a conclusion about the preferred route of the process, which makes it possible to find a set of kinetic constants for individual stages.

It is particularly important to know the route of a complex multi-stage process when predicting the behavior of an electrochemical system in which multi-stage processes occur on metals and alloys in the presence of surface-active organic additives of various nature. Interconnection between individual electrode reactions through intermediates is another important factor influencing the kinetics of such processes. Based on their regularities, it is possible to identify the role of the organic compound in the formation of electrochemical transformation products (for example, electrooxidation or electrodeposition) with specified characteristics. This is especially important for modern microelectronics since understanding the kinetics of complex multi-stage processes in electrolytes with organic surface-active additives contributes to determining optimal conditions for the formation of interconnections between elements of integrated circuits by the void-free filling of holes in the dielectric with metal in the presence

of electrochemically active organic compounds with high adsorption capacity.

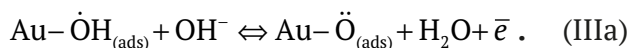
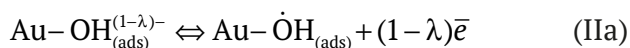
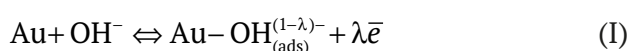
A typical example of a complex multi-step process is anodic oxidation of a monoaminoacetic acid (glycine) anion on an Au electrode in an aqueous alkaline solution. The areas of adsorption potentials and electrochemical activity of  $\text{Gly}^-$  and  $\text{OH}^-$  on gold overlap, which predetermines the potential for the mutual influence of partial reactions. In addition,  $\text{OH}^-$  anions [5–11] are directly involved in the heterogeneous electrooxidation reaction of the glycine anion. It is reasonable to assume that partial heterogeneous processes in the  $\text{Au}|\text{OH}^-, \text{H}_2\text{O}$  and  $\text{Au}|\text{Gly}^-, \text{OH}^-, \text{H}_2\text{O}$  systems will be kinetically coupled both due to the competition of  $\text{OH}^-$ ,  $\text{Gly}^-$ , intermediates and their electrooxidation products for active sites on the Au surface and due to the presence of common stages of the oxidation reactions of hydroxide and glycinate ions.

The purpose of this work was to use the method of graph-kinetic analysis to distinguish the partial oxidation currents of hydroxide ions and glycine anions during the general anodic process occurring on gold in an alkaline glycine-containing solution. It is possible that this will allow answering, at least qualitatively, the basic question: whether the kinetics of the anodic destruction of the glycine anion is its own or subordinate to the regularities of electrooxidation of hydroxide ions.

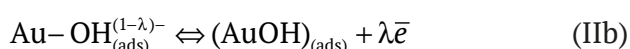
## 2. Calculation procedure

*Selecting the reaction scheme.* To use the graph-kinetic method successfully, it is necessary to construct a detailed kinetic reaction scheme.

The process of anodic oxidation of  $\text{OH}^-$  on gold in an aqueous medium has several stages. According to numerous researches [12–21], it proceeds via the chemisorption stage of the anion, most likely with partial charge transfer, and is accompanied by the sequential formation of mono- and biradical forms of adsorbed atomic oxygen. Earlier, we used the method of kinetic diagrams to analyze partial anodic processes in the  $\text{Au}|\text{OH}^-, \text{H}_2\text{O}$  system. The shape of the general stationary voltammogram was determined by calculation. A possible reaction scheme for the electroconversion of  $\text{OH}^-$  ion is:



Here,  $\lambda$  is the degree of partial charge transfer from an adsorbed particle with a charge  $z = 1$  per metal; eventually  $z_{\text{ads}} = 1 - \lambda$  [21]. It is assumed [22–24] that the radical ion state is stabilized due to the overlap of  $6s$ - and  $sp^3$ -AO for Au and  $\text{OH}^-$ , respectively. However, the appearance of 2D Au(I) and Au(II) compounds on the surface is possible in such processes as:



The formation of the phase Au(III) oxide at sufficiently high potentials can be the result of a process involving  $\text{Au}-\ddot{\text{O}}_{(\text{ads})}$  or  $(\text{AuO})_{\text{ads}}$ :



When choosing between alternative routes for anodic formation of  $\text{Au}_2\text{O}_3$ : via (IIa), (IIIa), and (IVa) or (IIb), (IIIb), and (IVb) stages, we preferred the first scenario due to the results of quantum chemical modeling. Therefore, this scenario was used later on, during the stage of constructing graphs for the intermediates of heterogeneous

processes of  $\text{OH}^-$  oxidation in the aqueous medium  $\dot{\text{O}}\text{H}$  and  $\ddot{\text{O}}$ .

The potential range of anodic release of molecular oxygen, which further complicates oxide formation on gold in an alkaline medium, was not considered in the study.

The main current maxima on the voltammogram of glycine anion oxidation have more positive values than the adsorption current maxima in the  $\text{Au}|\text{OH}^-, \text{H}_2\text{O}$  system [6, 10, 30, 31], however, they have noticeably more negative values than the  $\text{Au}_2\text{O}_3$  peak (Fig. 1). According to [6], the six-electron, generally anodic, process goes through the stage of dissociative  $\text{Gly}^-$  chemisorption, the products of which,  $(-\text{NH}_2\dot{\text{C}}\text{H}_2$  and  $-\text{COO}^-)$ , are then anodically oxidized to  $\text{CN}^-$ ,  $\dot{\text{N}}\text{H}_2$ , and  $\text{CO}_2$ . According to the method of a rotating ring-disc electrode [28], at  $E > 0.35$  V, adsorbed methylamine can also be formed. However, the results of *in situ* FTIR reflection spectroscopy [5, 6] indicate that the main intermediates of anode destruction of Gly on polycrystalline gold are formate ions. What is more, this method did not detect the formation of methylamine. In addition, the absorption bands corresponding to  $\text{CN}^-$ ,  $\text{OCN}^-$ , and  $\text{CO}_2$ , as well as  $\text{Au}(\text{CN})_2^+$  were reliably recorded. Taking into account these data, the putative scheme of the glycine anion oxidation, which reflects the features of the anodic transformation of  $\text{OH}^-$  and the possibility of coupling of individual reactions, is as follows:

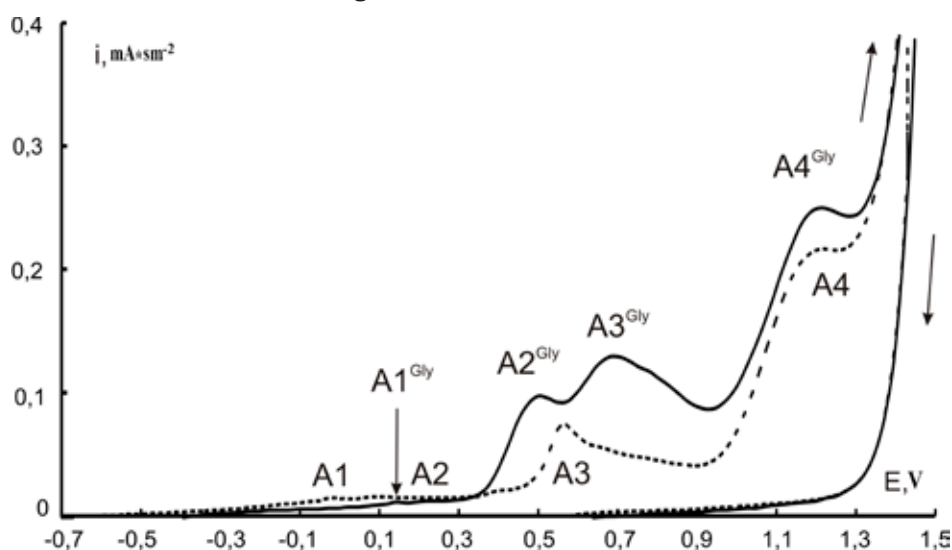


**Fig. 1.** Cyclic voltammograms obtained on a gold electrode in a background solution (dotted line) and with the addition of 0.03 M glycine;  $v = 0.10$  B/c [10]



$$k_{ji} = k_{ji}^0(E^0)c_j^v \exp[-(1-\lambda)\alpha F(E - E^0)/RT]. \quad (5b)$$

Here,  $E$  and  $E^0$  are the current and standard electrode potentials for a given reaction;  $\alpha$  and  $\beta$  are cathodic and anodic charge transfer coefficients (hereinafter  $\alpha = \beta = 0.5$ ). If the adsorption of a charged particle is not accompanied by a redistribution of electron density, then the influence of  $E$  on the rate constants in equations (4a), (4b), (5a), and (5b) disappears, and formulas (5a) and (5b) take their usual form. It is obvious that in the general case the values of  $K_{ij}$ ,  $K_{ji}$  also depend on the potential, although to varying degrees.

### 3. Analysis of kinetic diagrams

*Au|OH, H<sub>2</sub>O system.* Let us assume that the anodic processes occurring in gold in an alkaline background electrolyte are stationary. Such an assumption is necessary at this stage, since it is extremely difficult to obtain a complete equation for the nonstationary anodic voltammogram, including the potential range of all current maxima even in the background electrolyte solution. The task is even more complicated if, along with the oxidation of hydroxide ions, the electrooxidation of the glycine anion occurs in the same potential range. According to the analysis technique proposed in [1-4], a kinetic diagram of the anodic process on the Au electrode in a background alkaline electrolyte can be constructed as follows (Fig. 2). Here, the initial state (1) is the free active site of the gold surface initially occupied by a water molecule; the vertices of the graph correspond to the successive transformation of the OH<sup>-</sup> ion: Au-OH<sub>ads</sub><sup>-</sup>, Au-ÖH<sub>ads</sub>, Au-Ö<sub>ads</sub> and Au<sub>2</sub>O<sub>3</sub>. The covering of the surface with each type of adsorption centers is, respectively,  $\Theta_1, \Theta_2, \Theta_3, \Theta_4$ ,

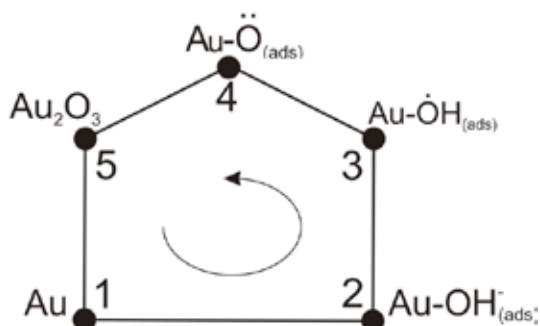
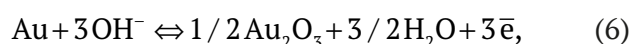


**Fig. 2.** Graph-kinetic diagram of adsorption and electrochemical processes occurring on an Au electrode in an alkaline medium in the region of potentials preceding the anodic release of molecular oxygen

and  $\Theta_5$ ; traversing the loop counterclockwise is positive. The overall reaction:



representing the sum of stages (I), (IIa), (IIIa), and (IVa), proceeds at the rate:

$$i_{15} = 3F(k_{15}\Theta_1 - k_{51}\Theta_5). \quad (7)$$

Each of these stages corresponds to the corresponding graph edge. To simplify the calculation procedure, the principle of the limiting stage was used, and kinetic situations with comparable speeds of two or more stages were not considered.

Let us assume that, for example, in the potential range of anodic peak A1 on the  $i, E$ -dependency (Fig. 1), the slowest is stage (I), while the rest of the stages are quasi-equilibrium. Since  $k_{12} \ll k_{ij}$  and  $k_{21} \ll k_{ij}$ , after a series of transformations, expression (7) can be represented in a fairly simple form:

$$i_{15} \approx i_{12} = 3F \left( \frac{k_{12}K_{23}K_{34}K_{45}K_{15}^{-1} - k_{21}}{1 + K_{23} + K_{23}K_{34} + K_{23}K_{34}K_{45} + K_{23}K_{34}K_{45}K_{15}^{-1}} \right). \quad (8)$$

In this case, the effect of kinetic coupling of individual stages is manifested through a change in values  $\Theta_1$  and  $\Theta_5$ , each of which is determined by a set of equilibrium constants from all stages of the process. It should be noted that under the procedure [2-4], expression (8) is written based on a fairly simple graphical algorithm, the structure of the graph is analyzed, and the system of equations (1)-(3) is not solved.

By subsequently assuming stages (IIa), (IIIa), and (IVa) as limiting, in a similar way we obtained expressions for the rate of the total oxidation reaction for gold in an alkaline medium in the potential range of peaks A2, A3, and A4:

$$i_{15} \approx i_{23} = 3F \left( \frac{k_{23} - k_{32}K_{54}K_{45}K_{21}K_{15}}{1 + K_{21} + K_{21}K_{15} + K_{21}K_{15}K_{54} + K_{21}K_{15}K_{54}K_{45}} \right) \quad (9)$$

$$i_{15} \approx i_{34} = 3F \left( \frac{k_{34}K_{23} - k_{43}K_{15}K_{21}K_{54}}{1 + K_{21} + K_{23} + K_{21}K_{15}K_{54} + K_{21}K_{15}} \right) \quad (10)$$

$$i_{15} \approx i_{45} = 3F \left( \frac{k_{45}K_{23}K_{34} - k_{54}K_{21}K_{15}}{1 + K_{21} + K_{23} + K_{23}K_{34} + K_{21}K_{15}} \right). \quad (11)$$

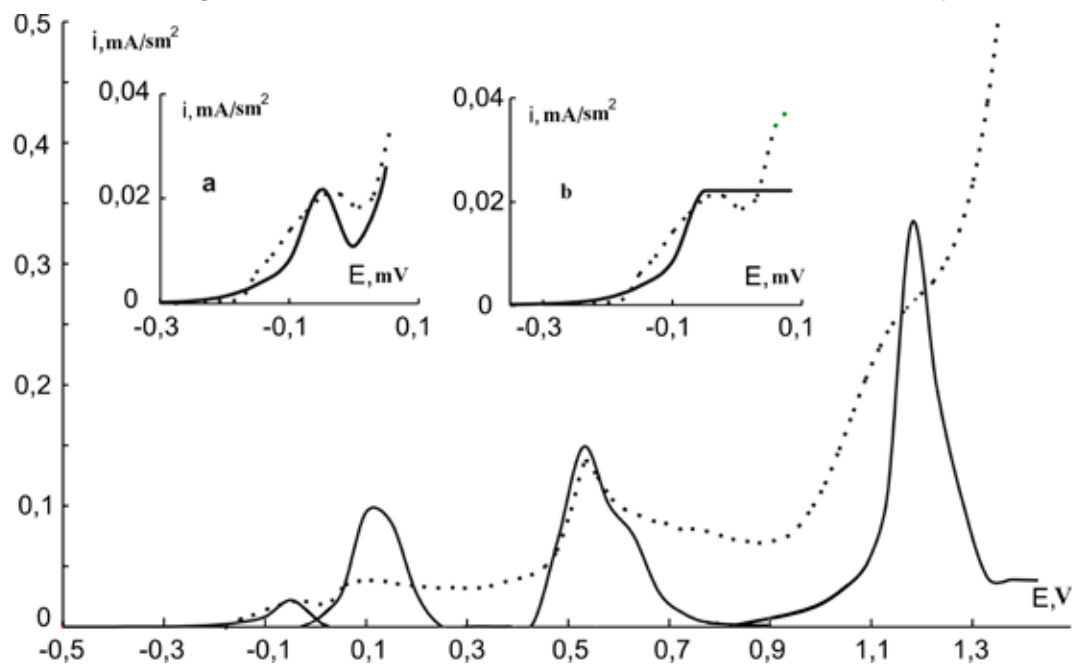
**Table 1.** Values of rate constants and equilibria constants of partial reactions occurring in the system Au|OH<sup>-</sup>,H<sub>2</sub>O

Constant	Edge of the graph				
	(1↔2)	(2↔3)	(3↔4)	(4↔5)	(5↔1)
$k_{ij}^0, \text{c}^{-1}$	$2.5 \cdot 10^{-7}$	$1.0 \cdot 10^{-9}$	$6.5 \cdot 10^{-1}$	$2.5 \cdot 10^{-4}$	–
$k_{ji}^0, \text{c}^{-1}$	$1.7 \cdot 10^{-13}$	$2.5 \cdot 10^{15}$	$4.3 \cdot 10^{21}$	$2.5 \cdot 10^{29}$	–
$K_{ij}^0$	$1.5 \cdot 10^6$	$4.0 \cdot 10^{-25}$	$1.5 \cdot 10^{-22}$	$1.0 \cdot 10^{-33}$	$9 \cdot 10^{-74}$

The sets of constants necessary for calculations were found by the brute force search based on the condition of best matching the position of each of the calculated and experimental anodic maxima. In addition, the values of the rate constants of direct and reverse reactions were determined (Table 1). It should be noted that the values of the equilibrium constants of individual stages by an order of magnitude coincided with the values of constants that could be calculated from known reference data [32]. The calculation showed that within the selected assumptions, the position of each of the four anodic current maxima on the calculated voltammogram correlated with the corresponding peak on the experimental  $i, E$ -dependence (Fig. 3). However, the A1 maximum on the calculated voltammogram could be obtained only by assuming  $\lambda \neq 0$ . Otherwise, in this potential range there is a horizontal

platform rather than a peak, which contradicts the experimental data (Fig. 3, inserts a and b).

Au| Gly<sup>-</sup>, OH<sup>-</sup>, H<sub>2</sub>O system. In the general case, the anodic processes in this system include the entire spectrum of reactions (I)–(XIII). Accordingly, the kinetic graph should consist of five interconnected cycles: anodic processes on Au in a background solution, the same, but with the addition of glycine, anodic reactions of additional oxidation of formate ions and cyanide ions, and dissolution of gold itself. However, the processes of OCN<sup>-</sup> and Au(CN)<sup>(5-)+</sup> formation occur at any noticeable rate only at high anodic potentials, that is why at this stage of the graph-kinetic analysis reactions (VIII) – (XIII) were not considered. The same applies to reactions (IVa) and (IVb) which correspond to the formation of gold oxide (III) at the potential of the A4 peak since its position and amplitude are practically insensitive to the


**Fig. 3.** The calculated voltammogram obtained in the Au|OH<sup>-</sup>,H<sub>2</sub>O system in comparison with the experimental one (dotted line). Inset: The maximum area A1, taking into account (a) and without taking into account the partial charge transfer (b) during the adsorption of the hydroxide ion

presence of glycine in the solution (Fig. 1). As a result, the kinetic analysis concerns only the potential range covering the anode peaks A1<sup>Gly</sup>, A2<sup>Gly</sup>, and A3<sup>Gly</sup>, i.e. it is limited to the study of coupled partial processes of adsorption and anodic oxidation of OH<sup>-</sup> and Gly anions and the additional oxidation of HCOO<sup>-</sup>. The graph corresponding to them contains three interconnected cycles: a, b, and c (Fig. 4A). However, it is also quite difficult to provide an analytical description of the processes within this graph, that is why further simplifications were made assuming that stages VI and VII proceed together. The resulting graph now contains only 2 cycles (Fig. 4B), in which the stage 1↔2 is common. Accordingly, the equilibrium constant  $K_{56}$  is multiplicative and is the product of the corresponding equilibrium constants of stages VI and VII. Therefore, it is impossible to separately determine the latter within the framework of this simplification.

It was assumed that in each cycle it was possible to distinguish a limiting stage in the

corresponding potential range, the kinetic regularities of which determine the shape of the partial anodic  $i, E$ -curve. It is reasonable to assume that, similar to the background electrolyte solution, with the growth of  $E$ , the nature of the limiting stage changes, so does the nature of the particles involved in the oxidation reactions in both cycles. The following most probable kinetic situations were considered:

*Kinetic route I.* In the potential range of the A1<sup>Gly</sup> – A2<sup>Gly</sup> maxima, the limiting stage in cycle **a** is (2↔3), and in cycle **b**, it is stage (5↔6). The total anodic current in this case should consist of partial currents of anodic oxidation of anions of hydroxyl  $i_{14}$  and glycine  $i_{17}$ \*

$$i_{14} = 2Fk_{25} \left( \frac{K_{12}(k_{52} + k_{67}k_{71})}{k_{52}k_{67}k_{71} \left( 1 + K_{21} + K_{14} + K_{71} + K_{14}K_{34} + K_{21}K_{52} + K_{67}K_{71} \right)} \right) \quad (12)$$

\* Although stage 1↔7 is an adsorption stage, the amount of adsorbate is determined by the rate of electrooxidation of glycine and additional oxidation of formate.

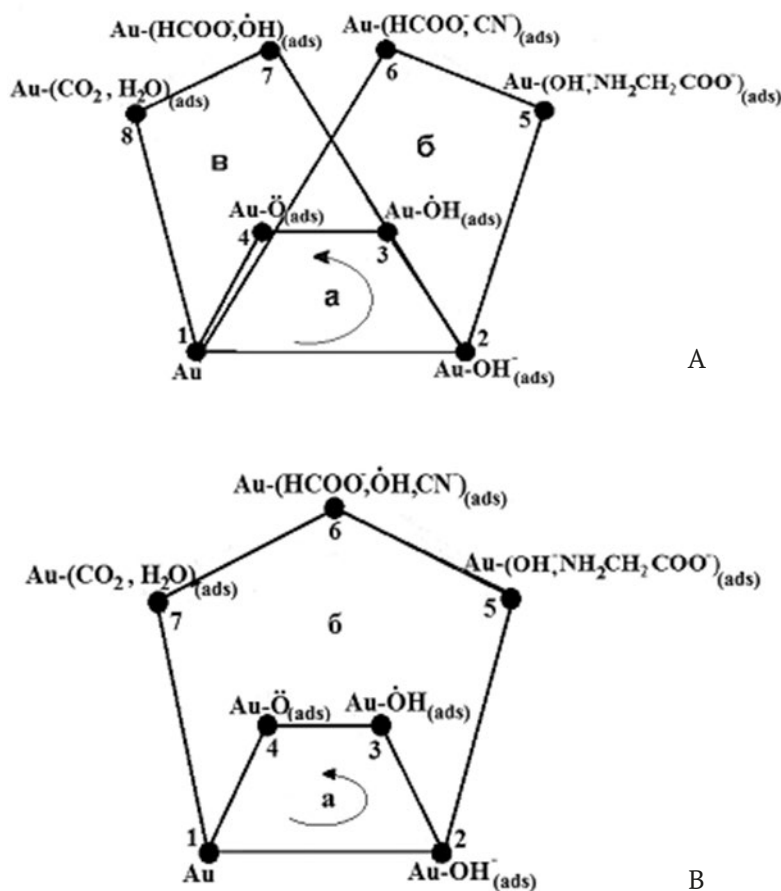


**Fig. 4.** General (A) and simplified (B) kinetic graphs of conjugated anode processes in the Au|Gly, OH<sup>-</sup>, H<sub>2</sub>O system in the region of anode maxima potentials A1<sup>Gly</sup> – A3<sup>Gly</sup>

$$i_{17} = 3Fk_{56} \left( \frac{K_{12}K_{25}}{1 + K_{21} + K_{14} + K_{71} + K_{14}K_{34} + K_{21}K_{52} + K_{67}K_{71}} \right). \quad (13)$$

*Kinetic Route II.* In the range of the A3<sup>Gly</sup> maximum, monoradicals are involved in the anodic process of cycle **a**  $\dot{O}H$ , while in cycle **b**, there is additional oxidation of formate ions. If in this case the limiting stages are (3 $\leftrightarrow$ 4) and (6 $\leftrightarrow$ 7), then:

$$i_{14} = 2Fk_{34} \left( \frac{K_{12}K_{23}}{k_{52}k_{65}k_{71} \left( 1 + K_{21} + K_{41} + K_{71} + K_{21}K_{32} + K_{21}K_{52} + K_{21}K_{52}K_{65} \right)} \right) \quad (14)$$

$$i_{17} = 3Fk_{67} \left( \frac{K_{12}K_{25}K_{56}(k_{41} + k_{32}k_{21})}{k_{52}k_{41} \left( 1 + K_{21} + K_{41} + K_{71} + K_{21}K_{32} + K_{21}K_{52} + K_{21}K_{52}K_{65} \right)} \right). \quad (15)$$

*Kinetic Route III.* Assuming that the nature of the limiting stage in cycle **b** does not change with the growth of the anode potential, i.e. the total current consists of the partial currents of the monoradical  $\dot{O}H$  and the glycine anion oxidation, processes (3 $\leftrightarrow$ 4) and (5 $\leftrightarrow$ 6) may be limiting. Wherein:

$$i_{14} = 2Fk_{34} \left[ \frac{K_{23}(k_{52} + k_{67}k_{71})}{k_{52}k_{67}k_{71}(1 + K_{21} + K_{23} + K_{25} + K_{21}K_{17} + K_{21}K_{14} + K_{21}K_{17}K_{76})} \right] \quad (16)$$

$$i_{17} = 3Fk_{56} \left[ \frac{K_{12}K_{25}(k_{41} + k_{32})}{k_{52}k_{41} \left( 1 + K_{21} + K_{23} + K_{25} + K_{21}K_{17} + K_{21}K_{14} + K_{21}K_{17}K_{76} \right)} \right]. \quad (17)$$

Since stages (2 $\leftrightarrow$ 5) and (1 $\leftrightarrow$ 7) are adsorption stages, they were not considered as limiting.

In all cases, the rate of the corresponding partial process is determined by the rate of its limiting stage, however, equations (12)–(17) have constants corresponding to the processes in both cycles, which actually reflects the effect of their mutual influence.

For the numerical calculation of partial currents, it is necessary to know the sets of the corresponding constants, the values of which were determined, as before, by brute force search. The starting point in determining the values of  $k_{ij}^o$ ,  $k_{ji}^o$ , and  $K_{ij}^o$  for partial background processes were the values of the constants given in Table 1. The brute force search procedure was completed when reaching the values of the sets of constants

that allowed matching the potentials' maxima of the calculated and experimental voltammograms.

The calculated partial voltammograms obtained under the assumption that there was any of the three possible kinetic situations are presented in Fig. 5 (a–d).

In the potential range of the A1 maximum, the introduction of the glycine anion led to an increase in the potential of the first maximum on the partial  $i, E$ -dependence corresponding to  $OH^-$  adsorption with partial charge transfer (as compared to the background solution), however, the rate of electrooxidation of  $Gly^-$  in the same potential range was negligibly small (Fig. 5a).

The A2 maximum on the partial curve in the  $Au|Gly^-, OH^-, H_2O$  system associated with the formation of  $\dot{O}H$  increased much more significantly as compared to the same maximum in the background solution (Fig. 5b). In this range, there was a process of glycine electrooxidation, the rate of which was maximum at  $E \approx 0.45$  V.

The anodic A3 maximum on the partial  $i, E$ -dependence corresponding to the electrooxidation of  $\dot{O}H$  and the formation of  $Au-\ddot{O}$  also increased in the presence of glycine, however, to a much smaller degree (Fig. 5c). Along with the electrooxidation of glycine, the process of formate ion additional oxidation was also possible. This process reached the maximum rate at  $E \approx 0.60$  V.

Finally, if we assume that the nature of the limiting stage for processes involving oxygen changes and for cycle **b** in any potential range the glycine electrooxidation reaction (5 $\leftrightarrow$ 6) is limiting, then the kinetic situation *III* is observed. The corresponding calculated partial  $i, E$ -dependencies are shown in Fig. 5d.

It is characteristic that the position of the maximum on the partial voltammogram corresponding to the process  $\dot{O}H \rightarrow \ddot{O}$ , remained practically unchanged (Fig. 5c and d). Whereas the maximum on the partial  $i, E$ -curve of glycine oxidation shifted considerably to the anodic region (Fig. 5b and d) and fell into the potential range of the anodic release of oxygen. The latter, however, contradicts the experimental data [10]. Therefore, we can come to the conclusion that in the  $Au|Gly^-, OH^-, H_2O$  system, with an increase in the anode potential, the kinetic situations *I* and *II* are consistently observed, which means that the nature of the limiting stages really changes.

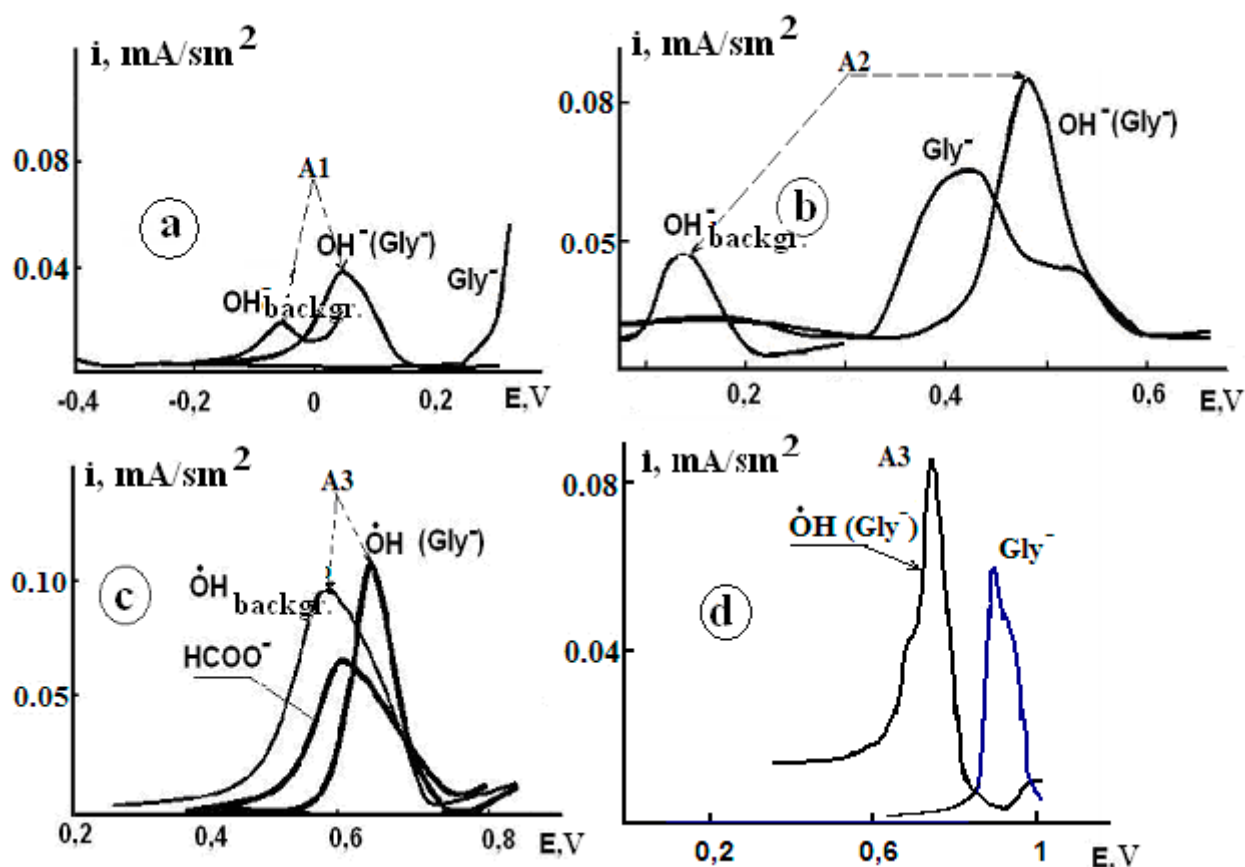


Fig. 5. Partial voltammograms calculated under the assumption that I (a-b); II (c) or III variant of the kinetic scheme (d) is realized

It is important that in any of the considered potential ranges, the rate of partial oxidation reactions for adsorbed  $\text{OH}$  and  $\text{OH}^-$  particles were significantly higher than that of electroactive organic particles. In the framework of formal kinetics of “parallel” reactions, this means that in the  $\text{Au}|\text{Gly}^-, \text{OH}^-, \text{H}_2\text{O}$  system, the kinetics of the glycine anion electroconversion was mainly determined by the kinetic features of the process of hydroxide ions electrooxidation.

The total voltammogram obtained by adding the partial  $i, E$ -characteristics of the processes involving  $\text{OH}^-$  and  $\text{Gly}^-$  is shown in Fig. 6. The insert to the figure shows a fragment for the potential range of the  $\text{A3}^{\text{Gly}}$  peak found under the assumption that kinetic situation III was observed. The discrepancy between the calculated and experimental  $i, E$ -dependence, both in terms of the maximum position and shape, once again confirms that this kinetic variant of Gly oxidation does not occur in practice.

With regards to variants I and II of the kinetic scheme, the position of the maxima on the

calculated and experimental voltamperograms practically coincided with each other. It is clear that in the potential range of the  $\text{A1}^{\text{Gly}}$  maximum, the overall rate of the process was determined only by the regularities of the electroconversion of oxygen on gold. In the range of the  $\text{A2}^{\text{Gly}}$  maximum, both the electro-oxidation reaction of  $\text{OH}^-$  ions and glycine anions contributed to the total current of the anodic process. Finally, the total anodic process at the  $\text{A3}^{\text{Gly}}$  potential consisted of three partial processes: the formation of an oxygen biradical, the electrooxidation of the formate ion, and the electrooxidation of glycine, which was oxidized in this region at a low but non-zero rate.

The rate and equilibrium constants of the processes occurring in cycles a and b calculated from the values of the sets of constants for partial reactions are presented in Table 2.

The analysis of these data showed that the values of the formal rate and equilibrium constants of electrochemical stages  $2 \rightleftharpoons 3$  and  $3 \rightleftharpoons 4$  for reactions with joint participation of  $\text{OH}^-$  and  $\text{Gly}^-$

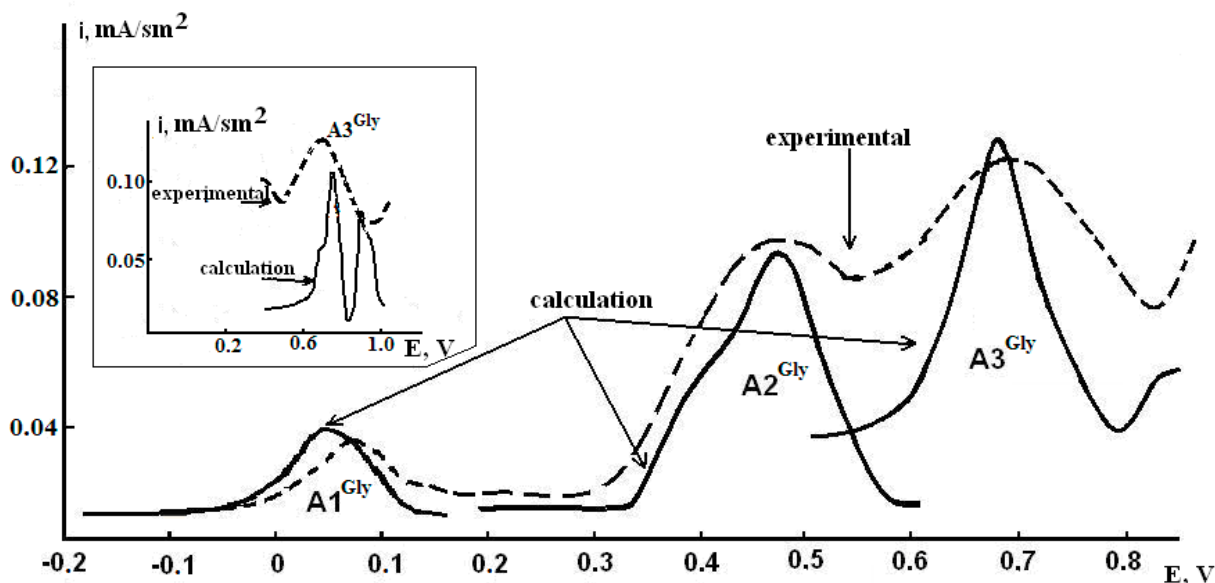


**Fig. 6.** Calculated total voltammogram obtained by graph-kinetic analysis under the assumption of the implementation of the I and II variants of the kinetic scheme; experimental  $i, E$ -dependence (dotted line). The inset is a fragment of the total  $i, E$ -dependence in the region of  $A3^{Gly}$  maximum potentials under the assumption of the implementation of the III variant of the kinetic scheme of the anodic oxidation process of the  $Gly^-$  anion

**Table 2.** Values of rate constants and equilibrium constants of partial reactions occurring in the  $Au|Gly^-, OH^-, H_2O$  system

Constant	Edge of the graph							
	1 $\leftrightarrow$ 2	2 $\leftrightarrow$ 3	3 $\leftrightarrow$ 4	4 $\leftrightarrow$ 1	2 $\leftrightarrow$ 5	5 $\leftrightarrow$ 6	6 $\leftrightarrow$ 7	7 $\leftrightarrow$ 1
$k_{ij}^0, c^{-1}$	$2.5 \cdot 10^{-2}$	$1.1 \cdot 10^{-9}$	$6.5 \cdot 10^{-1}$	$4.6 \cdot 10^{-22}$	$1.6 \cdot 10^4$	$6.0 \cdot 10^{-9}$	$6.0 \cdot 10^{-9}$	$9.0 \cdot 10^{-5}$
$k_{ji}^0, c^{-1}$	$4.2 \cdot 10^{-6}$	$9.7 \cdot 10^9$	$4.4 \cdot 10^{21}$	$2.1 \cdot 10^{-4}$	$1.0 \cdot 10^{-2}$	$7.2 \cdot 10^{-4}$	$7.0 \cdot 10^{-4}$	$1.3 \cdot 10^4$
$K_{ij}^0$	$5.8 \cdot 10^5$	$1.1 \cdot 10^{-19}$	$1.5 \cdot 10^{-22}$	$2.2 \cdot 10^{-18}$	$1.6 \cdot 10^6$	$8.3 \cdot 10^{-6}$	$8.5 \cdot 10^{-4}$	$6.9 \cdot 10^{-7}$

differ little from those obtained for the  $Au|OH^-, H_2O$  system, while the constants characterizing the process of hydroxide ion adsorption change significantly in the presence of glycine anion, which, in our opinion, once again indicates that the processes of electrooxidation of organic particles are governed by the kinetic regularities of anodic processes involving  $OH^-$  ions.

#### 4. Conclusions

1. The method of kinetic diagrams was used to analyze anodic processes in the  $Au|Gly^-, OH^-, H_2O$  system with a limited number of active sites on the gold surface. It was confirmed that partial multi-stage reactions of anodic oxidation of glycine and hydroxyl anions are kinetically coupled.

2. It was shown that with an increase in the anode potential, the nature of the limiting

stages of processes, both with the participation of background and organic particles, changes. Otherwise, the calculated  $i, E$  dependencies differ significantly from the experimental data.

3. Formal rate and equilibria constants of electrochemical reactions involving particles of background electrolyte and the position of the anodic maximum associated with the formation of an oxygen biradical are not very sensitive to the presence of  $Gly^-$  in the solution. However, the rates of partial oxidation reactions of adsorbed  $OH$  and  $\dot{O}H$  particles are significantly higher than those of organic anions ( $Gly^-$  and  $HCOO^-$ ). This indicates that the kinetics of the electrooxidation processes of  $Gly^{is}$  in the  $Au|Gly^-, OH^-, H_2O$  system are determined by the kinetic features of the electrooxidation reactions of hydroxide ions.

## Contribution of the authors

The authors contributed equally to this article.

## Conflict of interests

The authors declare that they have no known competing financial interests or personal relationships that could have influenced the work reported in this paper.

## References

1. Goldshtein B. N., Volkenshtein M. V. Investigation of nonstationary complex monomolecular reactions by the graph method\*. *Doklady of the USSR Academy of Sciences*. 1968;78: 386–388. (In Russ.)
2. Goldshtein B. N., Magarshak D. B., Volkenshtein M. V. Analysis of monosubstrate enzyme reactions by graph method\*. *Doklady of the USSR Academy of Sciences*. 1970;191: 1172–1174. (In Russ.)
3. Goldshtein B. N., Volkenshtein M. V. Simple kinetic models explaining critical phenomena in enzymatic reactions with enzyme and substrate isomerization\*. *Doklady of the USSR Academy of Sciences*. 1988;22: 1381–1392. (In Russ.)
4. Goldshtein B. N., Shevelev E. A., Volkenshtein M. V. Stability analysis of enzyme systems with feedbacks by the graph method\*. *Doklady of the USSR Academy of Sciences*. 1983;273: 486–488. (In Russ.)
5. Zhen C.-H., Sun S.-G., Fan C.-J., Chen S.-P., Mao B.-W., Fan Y.-J. In situ FTIRS and EQCM studies of glycine adsorption and oxidation on Au (111) electrode in alkaline solutions. *Electrochimica Acta*. 2004;49(8): 1249–1255. <https://doi.org/10.1016/j.electacta.2003.09.048>
6. Zhen Ch.-H. Adsorption and oxidation of glycine on Au film electrodes in alkaline solutions. *Acta Physico-Chimica Sinica*. 2003;19: 60–64. <https://doi.org/10.3866/pku.whxb20030114>
7. Beltowska-Brzezinka M., Uczak T., Holze R. Electrocatalytic oxidation of mono- and polyhydric alcohols on gold and platinum. *Journal of Applied Electrochemistry*. 1997;27: 999–1011. <https://doi.org/10.1023/a:1018422206817>
8. Štrbac S., Hamelin A., Adžić R. R. Electrochemical indication of surface reconstruction of (100), (311) and (111) gold faces in alkaline solutions. *Journal of Electroanalytical Chemistry*. 1993;362: 47–53. [https://doi.org/10.1016/0022-0728\(93\)80005-3](https://doi.org/10.1016/0022-0728(93)80005-3)
9. Chang S. C., Ho Y., Weaver M. J. Applications of real-time FTIR spectroscopy to the elucidation of complex electroorganic pathways: electrooxidation of ethylene glycol on gold, platinum, and nickel in alkaline solution. *Journal of the American Chemical Society*. 1991;113(25): 9506–9513. <https://doi.org/10.1021/ja00025a014>
10. Kraschenko T. G., Bobrinskaya E. V., Vvedenskii A. V., Kuleshova N. E. Kinetics of electrochemical oxidation of anion glycine on gold. *Condensed Matter and Interphases*. 2014;16(1): 42–49. (In Russ., abstract in Eng.). Available at: <https://www.elibrary.ru/item.asp?id=21490889>
11. Beltramo G. L., Shubina T. E., Koper M. T. M. Oxidation of formic acid and carbon monoxide on gold electrodes studied by surface-enhanced Raman spectroscopy and DFT. *ChemPhysChem*. 2005;6: 2597–2606. <https://doi.org/10.1002/cphc.200500198>
12. Martins M. E., Córdova O. R., Arvia A. J. The potentiodynamic electroformation and electroreduction of the O-containing layer on gold in alkaline solutions. *Electrochimica Acta*. 1981;26: 1547–1554. [https://doi.org/10.1016/0013-4686\(81\)85127-4](https://doi.org/10.1016/0013-4686(81)85127-4)
13. Bruckenstein S., Shay M. An in situ weighing study of the mechanism for the formation of the adsorbed oxygen monolayer at gold electrode *Journal of Electroanalytical Chemistry and Interfacial Electrochemistry*. 1985;188: 131–136. [https://doi.org/10.1016/s0022-0728\(85\)80057-7](https://doi.org/10.1016/s0022-0728(85)80057-7)
14. Burke L. D., Cunnane V. J., Lee B. H. Unusual postmonolayer oxide behavior of gold electrodes in base. *Journal of The Electrochemical Society*. 1992;139: 399–406. <https://doi.org/10.1149/1.2069230>
15. Vitus C. M., Davenport A. J. In situ scanning tunneling microscopy studies of the formation and reduction of a gold oxide monolayer on Au(111). *Journal of The Electrochemical Society*. 1994;141(5): 1291–1298. <https://doi.org/10.1149/1.2054912>
16. Goldshtein B. N., Zalkind Ts. I., Veselovskii V. I. Electrochemical adsorption of oxygen on a gold electrode in solutions of chloric and sulfuric acids\*. *Soviet Electrochemistry*. 1973;9(5): 699–702. (In Russ.)
17. Chen A., Lipkowski J. Electrochemical and spectroscopic studies of hydroxide adsorption at the Au(111) electrode. *The Journal of Physical Chemistry B*. 1999;103: 682–691. <https://doi.org/10.1021/jp9836372>
18. Vetter K. J. *Elektrochemische kinetik*. Springer Berlin, Heidelberg; 1961. <https://doi.org/10.1007/978-3-642-86547-3>
19. Tremiliosi-Filho G., Gonzalez E. R., Motheo A. J., Belgsir E. M., Léger J.-M., Lamy C. *Journal of Electroanalytical Chemistry*, 1998;444: 31–39. [https://doi.org/10.1016/S0022-0728\(97\)00536-6](https://doi.org/10.1016/S0022-0728(97)00536-6)
20. Nechaev I. V., Vvedenskii A. V. Quantum chemical modeling of hydroxide ion adsorption on group IB metals from aqueous solutions. *Protection of Metals and Physical Chemistry of Surfaces*. 2009;45(4): 391–397. <https://doi.org/10.1134/s2070205109040029>
21. Patritio E. M., Olivera P. P., Sellers H. The nature of chemisorbed hydroxyl radicals. *Surface Science*. 1994;306: 447–458. [https://doi.org/10.1016/0039-6028\(94\)90085-x](https://doi.org/10.1016/0039-6028(94)90085-x)

22. Alonso C., Gonzalez-Velasco J. Study of the electrooxidation of 1,3-propanediol on a gold electrode in basic medium. *Journal of Applied Electrochemistry*. 1988;18: 538–545. <https://doi.org/10.1007/bf01022248>
23. Safronov A. U., Kristensen P. A. IR spectroscopic characteristics of the surface of the gold electrode in solutions with different pH\*. *Soviet Electrochemistry*. 1990;26(7): 869–873. (In Russ.)
24. Kirk D. W., Foulkes F. R., Graydon W. F. The electrochemical formation of Au(I) hydroxide on gold in aqueous potassium hydroxide. *Journal of The Electrochemical Society*. 1980;127(10): 1069–1076. <https://doi.org/10.1149/1.2129819>
25. Icenhower D. E., Urbach H. B., Harrison J. H. Use of the potential-step method to measure surface oxides. *Journal of The Electrochemical Society*. 1970;117(12): 1500–1506. <https://doi.org/10.1149/1.2407359>
26. Štrbac S., Adžić R. R. The influence of OH- chemisorption on the catalytic properties of gold single crystal surfaces for oxygen reduction in alkaline solutions. *Journal of Electroanalytical Chemistry*. 1996;403: 169–181. [https://doi.org/10.1016/0022-0728\(95\)04389-6](https://doi.org/10.1016/0022-0728(95)04389-6)
27. Burke L. D. Scope for new applications for gold arising from the electrocatalytic behaviour of its metastable surface states. *Gold Bulletin*. 2004;37(1-2): 125–135. <https://doi.org/10.1007/bf03215520>
28. Dobberpuhl D. A., Johnson D. C. Pulsed electrochemical detection at ring of a ring-disk electrode applied to a study of amine adsorption at gold electrodes. *Analytical Chemistry*. 1995;67: 1254–1258. <https://doi.org/10.1021/ac00103a017>
29. Xiao Sun S.-G., Yao J.-L., Wu Q.-H., Tian Z.-Q. Surface-enhanced Raman spectroscopic studies of dissociative adsorption of amino acids on platinum and gold electrodes in alkaline solutions. *Langmuir*. 2002;18: 6274–6279. <https://doi.org/10.1021/la025817f>
30. Burke L. D., Nugent P. F. The electrochemistry of gold: II the electrocatalytic behaviour of the metal in aqueous media. *Gold Bull.* 1998;31: 39–49. <https://doi.org/10.1007/bf03214760>
31. Brown D. H., Smith W. E., Fox P., Sturrock R. D. The reactions of gold (0) with amino acids and the significance of these reactions in the biochemistry of gold. *Inorganica Chimica Acta*. 1982;(67): 27–30. [https://doi.org/10.1016/s0020-1693\(00\)85035-5](https://doi.org/10.1016/s0020-1693(00)85035-5)
32. Suhotin A. M. *Handbook of electrochemistry\**. Moscow: Khimiya Publ.; 1981. 487 p. (In Russ.)
- \* Translated by author of the article

### Information about the authors

Ilya D. Zartsyn, Dr. Sci. (Chem.), Professor of the Department of Physical Chemistry of the Voronezh State University (Voronezh, Russian Federation).

zar-vrn@mail.ru

Alexander V. Vvedenskii, Dr. Sci. (Chem.), Full Professor of the Department of Physical Chemistry of the Voronezh State University (Voronezh, Russian Federation).

<https://orcid.org/0000-003-2210-5543>

alvved@chem.vsu.ru

Elena V. Bobrinskaya, Cand. Sci. (Chem.), Associate Professor of the Department of Physical Chemistry of the Voronezh State University (Voronezh, Russian Federation).

<https://orcid.org/0000-0001-7123-4224>

elena173.68@mail.ru

Oleg A. Kozaderov, Dr. Sci. (Chem.), Docent, Head of the Department of Physical Chemistry, Voronezh State University (Voronezh, Russian Federation).

<https://orcid.org/0000-0002-0249-9517>

ok@chem.vsu.ru

Received 10.04.2023; approved after reviewing 19.04.2023; accepted for publication 15.06.2023; published online 25.06.2024.

Translated by Irina Charychanskaya